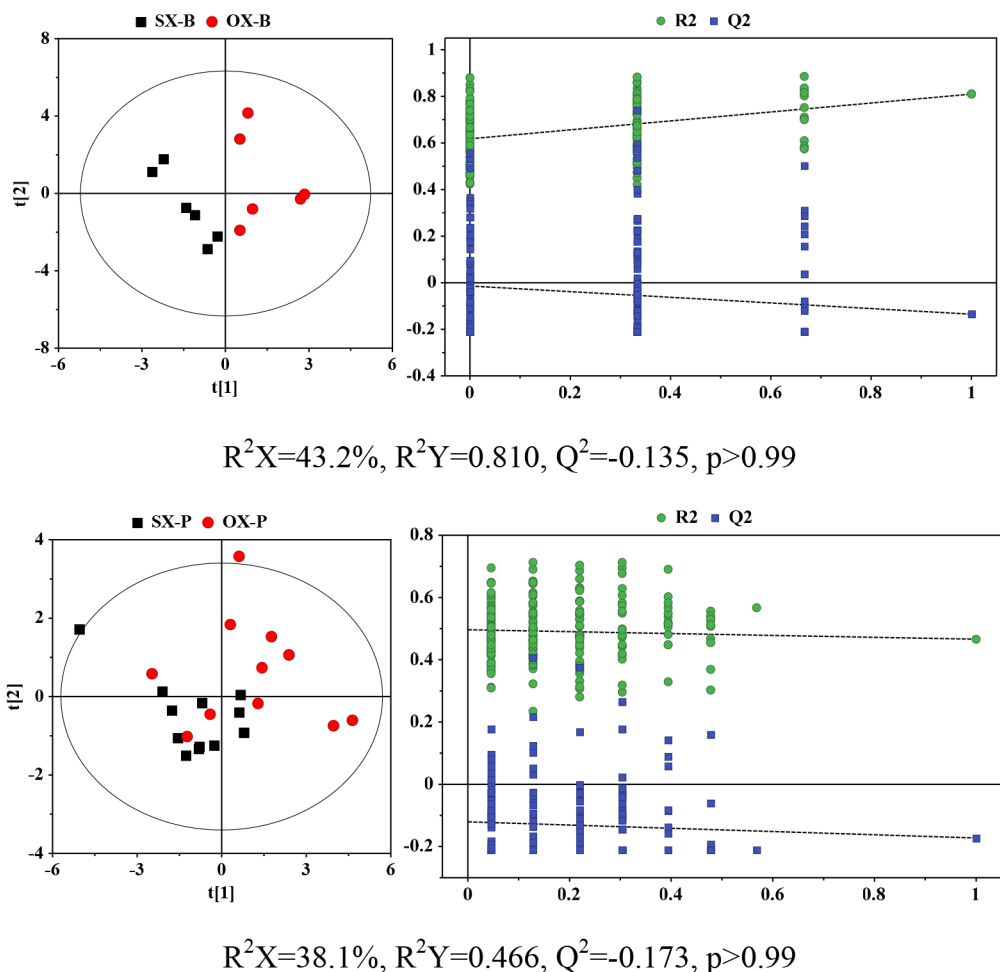
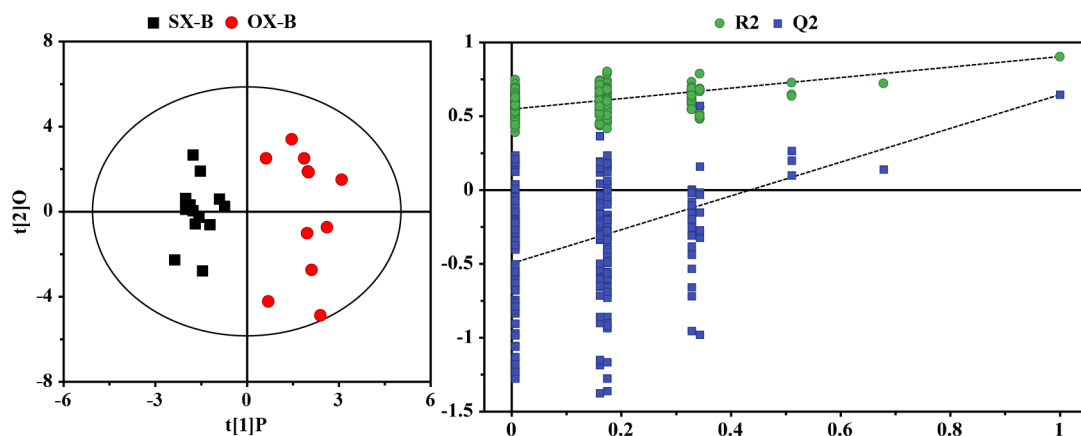


Identification and causes of metabonomic difference between orthotopic and subcutaneous xenograft of pancreatic cancer

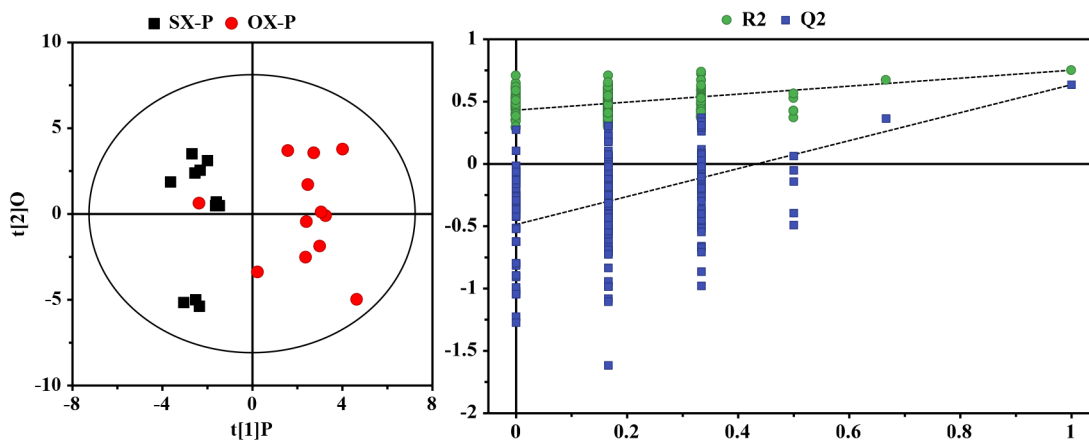
SUPPLEMENTARY MATERIALS



Supplementary Figure 1: OPLS-DA scores plots (left panels), the corresponding permutation plots (n=200) (right panels) and the results from CV-ANOVA (the p values) for serum profiles between subcutaneous xenograft (SX) and orthotopic xenograft (OX) groups induced by BxPC-3 cell strain (B) and Panc-1 cell strain (P).

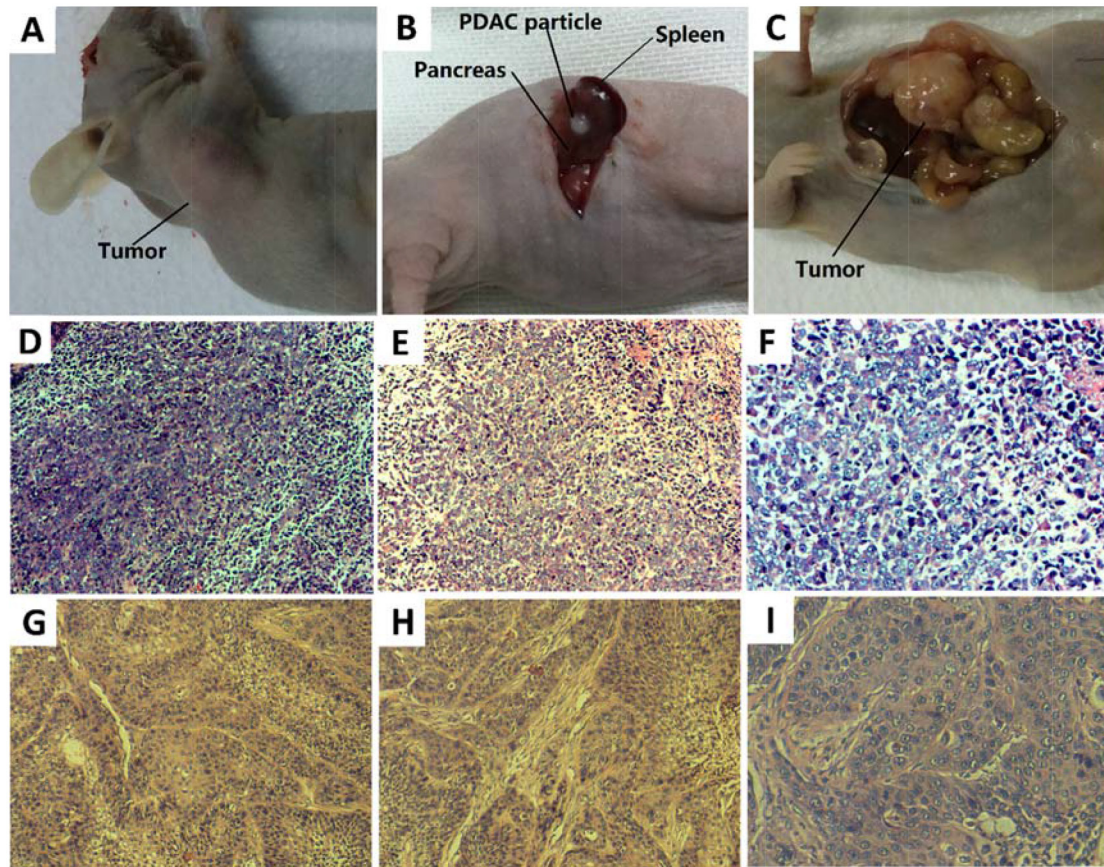


$R^2X=32.6\%$, $R^2Y=0.902$, $Q^2=0.643$, $p<0.001$



$R^2X=55.9\%$, $R^2Y=0.749$, $Q^2=0.632$, $p<0.001$

Supplementary Figure 2: OPLS-DA scores plots (left panels), the corresponding permutation plots (n=200) (right panels) and the results from CV-ANOVA (the p values) for tissue profiles between subcutaneous xenograft (SX) and orthotopic xenograft (OX) groups induced by BxPC-3 cell strain (B) and Panc-1 cell strain (P).



Supplementary Figure 3: The representative images of subcutaneous xenograft (SX) and orthotopic xenograft (OX) models induced by BxPC-3 cell strain (B) and Panc-1 cell strain (P) and corresponding histological observation. (A) the representative images of successful establishment of SX models, four weeks after operation. **(B)** The diagrammatic drawing of implantation of PDAC particles on the body and tail of pancreas. **(C)** The representative images of successful establishment of OX models. **(D)** (100 fold, H&E staining) the histological observation of tumor tissue derived from SX-P. **(E)** (100 fold, H&E staining) the histological observation of tumor tissue derived from OX-P. **(F)** (200 fold, H&E staining) the histological observation of tumor tissue derived from OX-P. **(G)** (100 fold, H&E staining) the histological observation of tumor tissue derived from SX-B. **(H)** (100 fold, H&E staining) the histological observation of tumor tissue derived from OX-B. **(I)** (200 fold, H&E staining) the histological observation of tumor tissue derived from OX-P. Images D-F and G-I confirmed that typical undifferentiated and moderate to well differentiated tumors were successfully established, respectively.